ELSEVIER

Journal of Nuclear Materials 297 (2001) 332–340

journal of nuclear materials

www.elsevier.com/locate/jnucmat

Thermodynamics of the UO_2 solid solution with magnesium and europium oxides

Takeo Fujino [a,1], Nobuaki Sato [a,*,1], Kohta Yamada [a,1], Shohei Nakama [a,1], Kousaku Fukuda [b,2], Hiroyuki Serizawa [b,2], Tetsuo Shiratori [b,2]

[a] *Institute for Advanced Materials Processing, Tohoku University, 2-1-1 Katahira, Aoba-ku, Sendai 980-8577, Japan*

[b] *Japan Atomic Energy Research Institute, Tokai Research Establishment, Tokai-mura, Naka-gun, Ibaraki-ken 319-1195, Japan*

Received 18 January 2001; accepted 15 May 2001

Abstract

Magnesium–europium solid solutions of uranium dioxide, $Mg_yEu_zU_{1-y-z}O_{2+x}$, with $y = 0.05$, 0.1 and $z = 0.05$, 0.1 were prepared, and their oxygen potential, $\Delta\bar{G}_{O_2}$, was measured as a function of O/M ratio (M = Mg + Eu + U) at temperatures of 1000°C, 1100°C and 1200°C. The O/M ratio which gave the steepest change of $\Delta\bar{G}_{O_2}$ (referred to as GOM) was 1.955 for $y = 0.05$, $z = 0.1$ (and $y = 0.05$, $z = 0.05$), but it decreased to 1.908 at higher Mg^{2+} concentrations of $y = 0.1$, $z = 0.05$. The GOM did not change with temperature in the range 1000–1200°C. The solid solutions showed distinct $\Delta\bar{S}_{O_2}$ peaks of near 0 J mol^{-1} K^{-1} at GOM, which was the same for $\Delta\bar{H}_{O_2}$ though the peaks were much smaller. The rates $\partial a/\partial y$ and $\partial a/\partial z$ for the lattice parameter change were −0.162 and −0.154 Å, respectively. At GOM, the Mg^{2+} ions of a fraction of 0.473 of total Mg^{2+} ions occupy the interstitial position of the fluorite lattice. The averaged numbers of U^{5+} ions bonded to one Mg^{2+} ion, α, were very small, i.e. 0.1–0.4. The large leftward shift in the curves of $\Delta\bar{G}_{O_2}$ vs. O/M ratio for this quarternary solid solution was considered to be caused by these small α values. © 2001 Elsevier Science B.V. All rights reserved.

PACS: 28.41.Bm

1. Introduction

Magnesium dissolves in uranium dioxide forming solid solution on heating the oxide solid mixture under suitable reaction conditions. The thermodynamic properties of this solid solution are not so simple [1–3]. In oxygen partial pressures of about 1 Pa, the solid solution is of substitutional type and the solubility of magnesium is as high as $y = 0.33$ with the formula $Mg_yU_{1-y}O_{2+x}$ [4,5], whereas the solubility decreases with decreasing oxygen partial pressure. If the oxygen partial pressure continues to decrease to 10^{-6} Pa, however, the solubility turns into an increase up to about $y = 0.1$ [6]. In this state, a part of the magnesium ions occupy the interstitial sites of the fluorite structure (4b position in space group $Fm\bar{3}m$) [7,8].

Uranium dioxide doped with magnesium is expected to show better fuel performance during irradiation until high burnups. First, it is supposed to exhibit more preferable thermodynamic properties of less susceptibility to the accumulated fission products, the amount of which is considerable at high burnups. The dissolved magnesium would lessen the oxygen potential change by the fission products. Second, the addition of a small amount of MgO in UO_2 is known to increase the grain size in the fuel pellets on fabrication. Then, if the diffusion coefficients of the fission gases do not change greatly by the dissolution of MgO, the release rate of the fission gases from the magnesium doped pellets decreases due to longer paths to attain grain boundaries. A large reduction factor of 2.5 has been obtained for UO_2

* Corresponding author. Tel.: +81-22 217 5163; fax: +81-22 217 5164.

E-mail address: dragon@tagen.tohoku.ac.jp (N. Sato).

[1] Tel.: +81-22 217 5163; fax: +81-22 217 5164.

[2] Tel.: +81-29 282 5404; fax: +81-29 282 6441.

0022-3115/01/$ - see front matter © 2001 Elsevier Science B.V. All rights reserved.
PII: S0022-3115(01)00627-4

doped with 5 mol% MgO [9,10]. The measured diffusion coefficient of ^{133}Xe for the UO_2 pellet doped with 3.4 mol% MgO did not alter significantly from that of the undoped UO_2 pellet [11].

The use of europium solid solution, $Eu_yU_{1-y}O_{2+x}$, as a burnable poison fuel has been discussed in the same way as gadolinium solid solution which is usually used for this purpose. The neutron cross-section of ^{151}Eu (isotopic abundance 48%) is large in the epithermal region. The oxygen potential ($\Delta\bar{G}_{O_2}$) of europium solid solution has been measured [12–17]. It shows a significant increase with the addition of europium. Also, the steepest change of $\Delta\bar{G}_{O_2}$ occurred at the O/M ratios in the range of $O/M < 2$ similar to the $\Delta\bar{G}_{O_2}$ behavior of magnesium solid solution. For $Eu_yU_{1-y}O_{2+x}$ of $y = 0.3$, the steepest change takes place at $O/M = 1.974$ at 1400°C [17].

This work was undertaken in order to study the change of thermodynamic properties of europium solid solution when magnesium is doped to it. Namely, the aim of the present work is to know whether the fuel performance of europium solid solution, which is possibly used as a burnable poison fuel, could be improved in a thermodynamical sense by the addition of magnesium. As for magnesium–gadolinium solid solution, $Mg_yGd_zU_{1-y-z}O_{2+x}$, $\Delta\bar{G}_{O_2}$ has already been measured. According to the result, the O/M ratio for the steepest $\Delta\bar{G}_{O_2}$ change lowered largely with increasing concentration of magnesium, whereas the ratio did not change with temperature in the range 1000–1200°C [8]. The above behavior for $Mg_yGd_zU_{1-y-z}O_{2+x}$ should be compared with $\Delta\bar{G}_{O_2}$ for $Mg_yEu_zU_{1-y-z}O_{2+x}$. For each of magnesium solid solution and europium solid solution, a number of oxygen potential data have been reported. Then, the thermodynamic properties of the present $Mg_yEu_zU_{1-y-z}O_{2+x}$ solid solution were discussed in comparison with these data.

2. Experimental

2.1. Materials used

Uranium metal turnings were dissolved in 6 M nitric acid, and uranium was purified by extracting into 100% TBP, where the impurity metals were left in the aqueous phase. The extracted uranium was scrubbed first with water and then with dilute ammonium carbonate solution. By adding ammonium hydroxide, ammonium diuranate precipitate was formed which was filtrated using a G4 glass filter under suction. After the precipitate was dried, it was converted to UO_3 by heating in air at 500°C [18]. Stoichiometric UO_2 was obtained by heating the UO_3 in a stream of hydrogen at 1000°C for 6 h. The main metallic impurities in UO_2 as analyzed with ICP method are shown in Table 1.

Table 1
Metallic impurities in UO_2

Element	Amount (ppm)
Pd	54
Y	2
La	4
Tm	94
Th	4

Heavy MgO of guaranteed reagent-grade ($CaO < 0.05\%$, heavy metals <0.005%) was purchased from Wako Pure Chemicals Industries Co. Europium sesquioxide with 99.9% purity was obtained from Nippon Yttrium. Hydrogen of extra high purity (nominally 99.999%) was produced with a Whatman Model 75-34JA-100 hydrogen generator. Carbon dioxide and N_2 (99.99%) gases were obtained from Nippon Sanso and used as received.

2.2. Preparation of solid solution

The calculated masses of MgO, Eu_2O_3 and UO_2 were intimately mixed in an agate mortar for about 40 min. The mixture was heated in air in a muffle furnace at 800°C for three days to obtain the oxides of magnesium–europium–uranium in an oxidized form. The cycle of mixing and heating was repeated three times in order to produce homogeneous products.

The air heated product (~1 g) was pressed into 10 mmϕ pellets, and heated on an alumina boat in a horizontal SiC tube furnace at 1250°C for two days in a stream of CO_2/H_2 mixed gas of which the mixing ratio was controlled to 450:1 ml min^{-1} with two mass-flow controllers (Kofloc, Type-3510 1/4 SW-500 SCCM and 1/4SW-10 SCCM). Calculation shows that the oxygen partial pressure of 1.0 Pa was obtained with this gas ratio at 1250°C [19]. After the reaction, the pellet was crushed and mixed. The mixture was heated again as pellets under the same conditions as mentioned above. The solid solutions formed were subjected to oxygen potential measurements after performing X-ray diffraction and chemical analyses.

2.3. X-ray diffraction analysis

X-ray powder diffractometry was carried out with a Rigaku Type RAD-IC diffractometer using CuKα radiation (40 kV, 20 mA) monochromatized with curved pyrolytic graphite. The slit system used was 1°–0.5 mm–1°–0.15 mm. The measurement was performed in the range $10° \leqslant 2\theta \leqslant 140°$ with a scanning rate of $1°(2\theta)$ min^{-1}. The cubic lattice parameter of the solid solution was calculated by the least-squares method using the LCR2 program [20]. The precipitation of MgO phase from solid solution was examined by step

scanning (18 s counting time and 0.01°(2θ) step width) in the range $40.88° \leqslant 2\theta \leqslant 44.88°$ to detect the strongest MgO peak which should appear at ~42.8°(2θ).

2.4. Chemical analysis

Solid solution powder (10–20 mg) was weighed with an accuracy of ±10 μg and dissolved in 5 ml Ce(IV) solution in 1.5 M sulfuric acid by warming the solution. The x value of the solid solution was determined by titrating the remaining (excess) Ce (IV) with Fe(II) ammonium sulfate solution using ferroin indicator [21,22]. The concentrations of Ce(IV) and Fe(II) solutions used were obtained by titrating stoichiometric UO_2. The estimated standard deviation in the titrated x values is within ±0.005.

2.5. Oxygen potential measurement

2.5.1. Method 1

Solid solution powder (2–3 g) was pressed into pellets. The pellets with three different magnesium concentrations were placed on an aluminum boat. Subsequently, they were heated in a horizontal SiC resistance tube furnace in a stream of CO_2/H_2 mixed gas. The mixing ratio of the gases was controlled by means of two mass-flow controllers in order to attain the intended oxygen partial pressure, where the mixing ratio of the gases was calculated by the use of the literature ΔG_f° values for H_2O (g), CO_2 (g) and CO (g) [19]. The samples were heated at a fixed temperature and oxygen partial pressure for 3–4 days to attain equilibrium. After the reaction, the whole system was evacuated, and the current to the furnace was turned off. The O/M ratios of the cooled samples were determined by chemical analysis.

2.5.2. Method 2

The solid solution sample (400–800 mg), whose O/M ratio had been determined by chemical analysis, was precisely weighed. The sample in a quartz basket was suspended from a Cahn-RG electrobalance by a platinum wire. The whole system was evacuated with a rotary pump. After evacuating for 1 h, the stopcock connected to the rotary pump was closed, and no leakage of vacuum was found for several hours on a mercury manometer. Then, N_2 gas was slowly introduced into the system up to the ambient pressure. The CO_2/H_2 mixed gas was led to flow over the sample. The mixing ratio of the CO_2/H_2 gases was controlled with the mass-flow controllers to have an intended oxygen partial pressure at the heating temperature.

The sample was heated in a flow of the mixed gas. After no weight change of the sample was recorded for several hours, the mixing ratio of the gases was changed for the next measurement. For the measurements at a higher temperature, 1200°C, a platinum basket was used instead of quartz basket. Below the oxygen partial pressure of 10^{-11} Pa, nickel suspension wire and basket were used. After a series of experiments to measure the weights at various oxygen partial pressures were finished, the sample was equilibrated with the mixed gas of $p_{O_2} = 10^{-8}$ Pa at 1200°C, followed by evacuation with a rotary pump and furnace cooling. It is generally accepted that the solid solutions give the steepest change in the curve of $\Delta\bar{G}_{O_2}$ versus O/M ratio around this oxygen pressure at 1000–1200°C [23]. Therefore, after this O/M ratio was obtained in the thermogravimetric curve, the sample was cooled and chemical analysis was performed. The O/M ratios that had been measured by thermogravimetry were corrected using the O/M ratio for the steepest $\Delta\bar{G}_{O_2}$ change determined by titration.

3. Results and discussion

3.1. Oxygen potential as a function of O/M ratio

The $\Delta\bar{G}_{O_2}$ data for $Mg_yEu_{0.05}U_{1-y-0.05}O_{2+x}$ ($x \gtreqless 0$) measured by method 2 are plotted against O/M ratio in Fig. 1. The right two (1 and 2), middle two (3 and 4) and

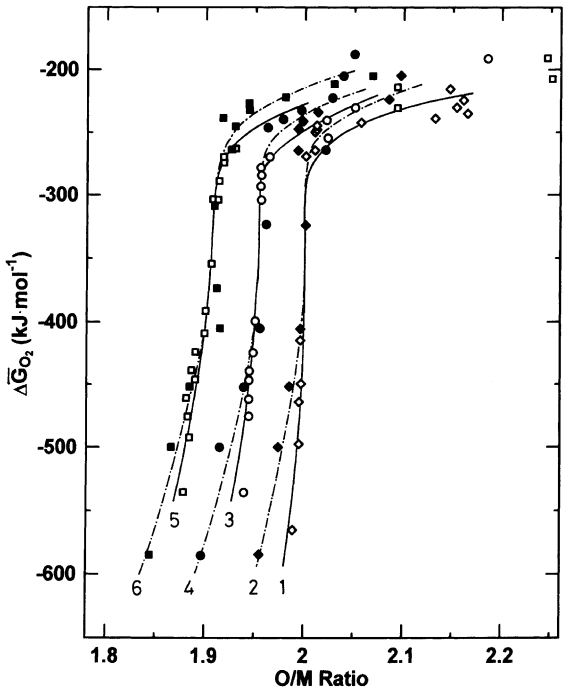

Fig. 1. Oxygen potential, $\Delta\bar{G}_{O_2}$, as a function of O/M ratio (M = Mg + Eu + U) for magnesium–europium solid solution, $Mg_yEu_zU_{1-y}O_{2+x}$, at 1000°C and 1200°C. Curves 1 and 2: $y = 0$, $z = 0.05$; Curves 3 and 4: $y = 0.05$, $z = 0.05$; Curves 5 and 6: $y = 0.1$, $z = 0.05$; Solid lines: 1000°C; Dash–dotted lines: 1200°C.

left two (5 and 6) curves indicate $\Delta\bar{G}_{O_2}$ for $y = 0$, 0.05 and 0.1, respectively. The solid and dash-dotted lines show the $\Delta\bar{G}_{O_2}$ change at 1000°C and 1200°C, respectively. From the figure, it is seen that the oxygen potential curve shifts leftward largely as the concentration of magnesium increases. This feature is the same as has been observed for $(Mg, Gd, U)O_{2+x}$ [8] and $(Mg, Ce, U)O_{2+x}$ [24] solid solutions. The oxygen potential of curves 2, 4 and 6 for 1200°C lowers more slowly than that of curves 1, 3 and 5 for 1000°C with decreasing O/M ratio below the O/M ratios which give rise to the steepest $\Delta\bar{G}_{O_2}$ change; the latter ratios will be referred to as GOM hereafter in this paper. Let us compare the O/M ratios at $\Delta\bar{G}_{O_2} = -600$ kJ mol^{-1}, for example. The O/M ratio for curve 2 ($y = 0$, 1200°C) is retrieved to be 1.95 from Fig. 1, which is lower than the GOM, viz. 1.995, by 0.045. On the other hand, the corresponding O/M ratio for curve 1 ($y = 0$, 1000°C) is 1.979. This value is lower than the GOM only by 0.016. In other words, the slope is much steeper for the 1000°C curve. However, it might be worthwhile to note that the curves obtained by thermogravimetry tend to give gentler slopes below GOM at 1000°C. In our earlier work, for europium solid solution [13], the oxygen potential was obtained by measuring the weight of the quenched sample with an ordinary microbalance after taking out from the furnace, where $\Delta\bar{G}_{O_2}$ for the europium concentration of 0.1 almost vertically decreased from $\Delta\bar{G}_{O_2} = -200$ to -500 kJ mol^{-1} both at 850°C and 1050°C. In method 2, there remains a possibility of small systematic error which gave slightly lower O/M ratios. The thermogravimetric measurements should be made for the samples in equilibrium with the oxygen partial pressures of the gas phase. However, it was often the case that the baseline of the thermogravimetry curve shifted on long time heating under the fixed experimental conditions, which made it difficult to have precise data. Then, the measurements were made after the equilibration time of about one day, though some change might appear in the slopes below GOM by this method [8]. Also, vaporization of metallic components in the sample during heating, if any, induces change in the O/M ratios, the effect of which is negligibly small in method 1.

Fig. 1 shows that the $\Delta\bar{G}_{O_2}$ curve shifts leftward with increasing magnesium concentration but it does not shift upward. This result means that the oxygen potential does not increase largely with the addition of magnesium if discussion on $\Delta\bar{G}_{O_2}$ is made after GOM is corrected to that of $y = 0$ for each solid solution containing magnesium. In addition to this, the GOM does not change with temperature in the range 1000–1200°C. These $\Delta\bar{G}_{O_2}$ properties are very similar to those observed for quaternary solid solutions $Mg_yGd_zU_{1-y-z}O_{2+x}$ [8] and $Mg_yCe_zU_{1-y-z}O_{2+x}$ [24]. On the other hand, some differences seem to be present when the $\Delta\bar{G}_{O_2}$ values of the present solid solution are compared with those of $Mg_yU_{1-y}O_{2+x}$ [3,4] and $Eu_yU_{1-y}O_{2+x}$ [13,15] solid solutions, for which the leftward shift of the $\Delta\bar{G}_{O_2}$ curve was accompanied by the significant $\Delta\bar{G}_{O_2}$ increase with the addition of magnesium or europium.

3.2. Partial molar entropy and enthalpy of oxygen as a function of O/M ratio

Partial molar entropy of oxygen, $\Delta\bar{S}_{O_2}$, was calculated from the temperature dependence of $\Delta\bar{G}_{O_2}$, assuming that $\Delta\bar{S}_{O_2}$ and partial molar enthalpy of oxygen, $\Delta\bar{H}_{O_2}$, are independent of temperature. This is nearly correct for most solid solutions [23]. Using the relation $\Delta\bar{S}_{O_2} = -\partial\Delta\bar{G}_{O_2}/\partial T$, $\Delta\bar{S}_{O_2}$ was calculated by dividing the difference $-\{\Delta\bar{G}_{O_2}(1200°C) - \Delta\bar{G}_{O_2}(1000°C)\}$ by 200 for each O/M ratio. The partial molar enthalpy of oxygen, $\Delta\bar{H}_{O_2}$, was obtained using the relation, $\Delta\bar{H}_{O_2} = \Delta\bar{G}_{O_2} + T\Delta\bar{S}_{O_2}$.

Fig. 2 shows the variation of $\Delta\bar{S}_{O_2}$ with O/M ratio. Curves 1, 2 and 3 in the figure express the $\Delta\bar{S}_{O_2}$ change for $y = 0$, 0.05 and 0.1 of $Mg_yEu_{0.05}U_{1-y-0.05}O_{2+x}$, respectively. It is seen from the figure that $\Delta\bar{S}_{O_2}$ for $y = 0$ does not change largely with O/M ratio in the range 2.01–2.08 showing the values near -50 J mol^{-1} K^{-1}.

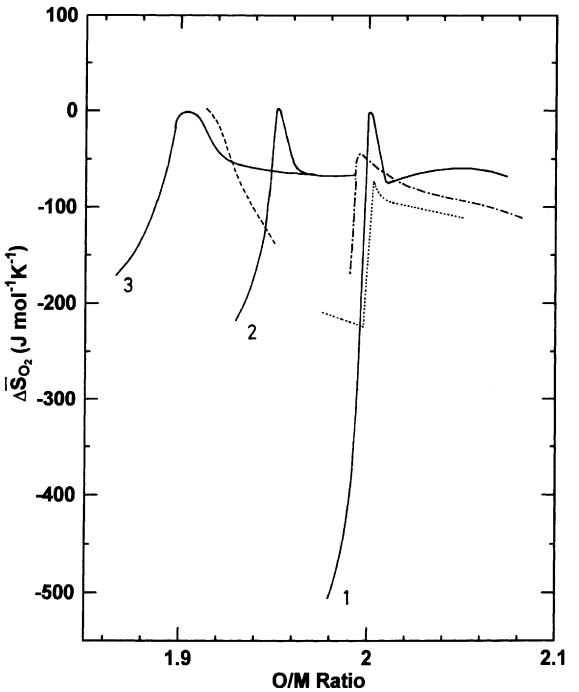

Fig. 2. Partial molar entropy of oxygen, $\Delta\bar{S}_{O_2}$, as a function of O/M ratio for $Mg_yEu_zU_{1-y-z}O_{2+x}$ (Dotted and broken lines for $Mg_yGd_zU_{1-y-z}O_{2+x}$). Curve 1: $y = 0$, $z = 0.05$; Curve 2: $y = 0.05$ $z = 0.05$; Curve 3: $y = 0.1$, $z = 0.05$; Dash-dotted line: $y = 0.05$, $z = 0$ [3]; Dotted line: $y = 0$, $z = 0.14$ [25]; Broken line: $y = 0.1$ $z = 0.142$ [8].

However, it increases as the O/M ratio decreases below 2.01, yielding a maximum of ~ 0 J mol^{-1} K^{-1} at O/M = 2.0. Then, the $\Delta\bar{S}_{O_2}$ curve rapidly decreases with decreasing O/M ratio. The present result is a little diverted from the earlier data for europium solid solutions where the distinct peak was not observed for $Eu_{0.05}U_{0.95}O_{2+x}$, although a sharp peak was observed for $Eu_{0.1}U_{0.9}O_{2+x}$ [15]. This difference is thought to be caused by a slight shift of the measured O/M ratios in the $\Delta\bar{G}_{O_2}$ curve. This effect on $\Delta\bar{S}_{O_2}$ is large at the O/M ratios in the vicinity of the peak position, because $\Delta\bar{S}_{O_2}$ values are calculated from the temperature dependence of the $\Delta\bar{G}_{O_2}$.

Curve 2 ($y = 0.05$) in Fig. 2 gives essentially the same trend as curve 1, but curve 2 is shifted leftward as a result of magnesium addition. The shift of curve 3 for $y = 0.1$ is larger with a broadened peak. For all three curves, the maximum values of $\Delta\bar{S}_{O_2}$ are near zero since the GOM does not change with temperature.

The present partial molar entropies can be compared with those of the other solid solutions. Curve 1 (Mg = 0, Eu = 0.05) of this work is seen to be in fairly good agreement with $\Delta\bar{S}_{O_2}$ of gadolinium solid solution (Gd = 0.14) reported by Une and Oguma [25] shown by dotted line, except that the O/M ratio giving the $\Delta\bar{S}_{O_2}$ peak is lower for the present solid solution (Mg = 0, Eu = 0.05) to a small extent. The $\Delta\bar{S}_{O_2}$ curve for magnesium solid solution (Mg = 0.05) [3] shown by dash-dotted line is also close to curve 1, although the peak position (O/M ratio) is distinctly lower than 2.0 for the magnesium solid solution. The reference broken line for $Mg_yGd_zU_{1-y-z}O_{2+x}$ (Mg = 0.1, Gd = 0.142) [8] does not show a peak. However, it would show one if the data acquisition is successfully made to the lower O/M ratio, since this curve is close to curve 3 of this work (Mg = 0.1, Eu = 0.05) which exhibits a maximum. It seems likely that the curve is basically prescribed by the concentration of magnesium. In [8], the concentration of gadolinium was 0.142, and in this work that of europium is 0.05. The two curves for these solid solutions with the same magnesium concentration (Mg = 0.1) are nearly overlapped.

The variation of $\Delta\bar{H}_{O_2}$ with O/M ratio is shown in Fig. 3. Curves 1, 2 and 3 depict $\Delta\bar{H}_{O_2}$ for $y = 0$, 0.05 and 0.1, respectively. These three curves show very small peaks at the same O/M ratios as those for the $\Delta\bar{S}_{O_2}$ peaks. Curve 1 is in fairly good agreement with the earlier $\Delta\bar{H}_{O_2}$ data for $Eu_{0.05}U_{0.95}O_{2+x}$ [15]. Nevertheless, some differences are seen in the range of O/M ratios above 2.0. The present curve turns into a slow increase as the O/M ratio increases after the small peak, while the reference curve continuously decreases after giving the peak.

In Fig. 3, both curves 2 and 3 for $y = 0.05$ and 0.1, respectively, are similar to curve 1. The O/M ratios for peaks in these curves are shifted leftward as a result of

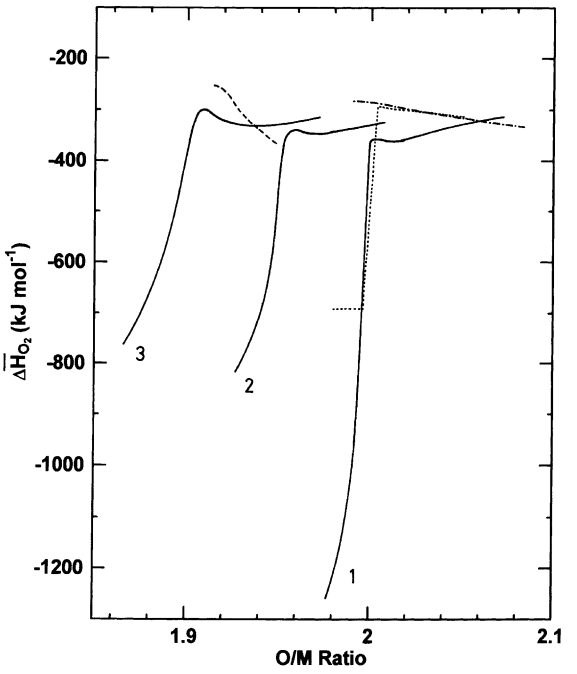

Fig. 3. Partial molar enthalpy of oxygen, $\Delta\bar{H}_{O_2}$, as a function of O/M ratio for $Mg_yEu_zU_{1-y-z}O_{2+x}$ (dotted and broken lines for $Mg_yGd_zU_{1-y-z}O_{2+x}$). Curve 1: $y = 0$, $z = 0.05$; Curve 2: $y = 0.05$, $z = 0.05$; Curve 3: $y = 0.1$, $z = 0.05$; Dash-dotted line: $y = 0.05$, $z = 0$ [3]; dotted line: $y = 0$, $z = 0.14$ [25]; Broken line: $y = 0.1$, $z = 0.142$ [8].

magnesium doping. On close examination, an increase in $\Delta\bar{H}_{O_2}$ at the peak tops was observed with increasing concentration of magnesium. Also, the slope in the region of O/M ratio lower than that which gives the $\Delta\bar{H}_{O_2}$ peak became gentler with the increase of magnesium concentration.

Curve 1 is in accord with the $\Delta\bar{H}_{O_2}$ curve for magnesium solid solution (Mg = 0.05) [3] shown by dash-dotted line in Fig. 3. Also, the curve is well consistent with the $\Delta\bar{H}_{O_2}$ curve for gadolinium solid solution with Gd = 0.14, shown by dotted line [25]. These reference curves, however, decrease with increasing O/M ratio at higher O/M ratios. The reason for this slight discrepancy is unclear at present. Curve 3 of this work is comparable with the broken line for the quaternary solid solution of Mg = 0.1 and Gd = 0.142 [8]. It can be suggested that the feature of the curve is primarily prescribed by the magnesium concentration with small modification by the coexisting lanthanide element metals.

3.3. GOM dependence on temperature

The GOM change with temperature was studied by method 1. The obtained data are listed in Table 2. In this

Table 2
$\Delta\bar{G}_{O_2}$, O/M ratios and lattice parameters at the steepest change of $\Delta\bar{G}_{O_2}$

Heating no.	Mg (y)	Eu (z)	Temp. (°C)	$p(O_2)$ (Pa)	$\Delta\bar{G}_{O_2}$ (kJ mol^{-1})	O/M ratio	a (Å)	Remarks[a]
1	0.05	0.05	1000	3.4×10^{-8}	−303.9	1.955	5.4624 ± 0.0001	S, s
2	0.05	0.05	1050	10^{-8}	−380.0	1.954		
3	0.05	0.05	1100	10^{-10}	−394.3	1.904		
4	0.05	0.05	1100	10^{-8}	−341.7	1.964	5.4604 ± 0.0003	S, s
5	0.05	0.05	1200	2.1×10^{-9}	−385.7	1.959	5.4637 ± 0.0002	S, s
1	0.1	0.05	1000	3.4×10^{-8}	−303.9	1.906	5.4581 ± 0.0001	S, b
2	0.1	0.05	1050	10^{-8}	−380.0	1.941		
3	0.1	0.05	1100	10^{-10}	−394.3	1.950		
4	0.1	0.05	1100	10^{-8}	−341.7	1.913	5.4611 ± 0.0002	S, s
5	0.1	0.05	1200	2.1×10^{-9}	−385.7	1.911	5.4579 ± 0.0005	S, sb
1	0.05	0.1	1000	3.4×10^{-8}	−303.9	1.954	5.4543 ± 0.0001	S, sb
5	0.05	0.1	1200	2.1×10^{-9}	−385.7	1.954	5.4549 ± 0.0002	S, s

[a] S: Fluorite single phase, s: Sharp X-ray diffraction peaks, sb: Somewhat broad X-ray diffraction peaks, b: Broad X-ray diffraction peaks.

series of experiments, the samples were heated at the intended temperature for longer periods of 4–5 days to attain equilibrium.

The GOM data are plotted against temperature in Fig. 4, where the marks ○, ●, and □ show the measured values for solid solutions of $y = 0.05$, $z = 0.05$; $y = 0.05$, $z = 0.1$ and $y = 0.1$, $z = 0.05$, respectively. The O/M ratio, 1.954, for $y = 0.05$, $z = 0.1$ solid solution at 1000°C is not shown in the figure, because of the overlap of the value with that for $y = 0.05$, $z = 0.05$ solid solution. The value O/M = 1.880 for $y = 0.1$, $z = 0.05$ solid solution at 1000°C in Fig. 4 is that from the heating experiment other than those given in Table 2.

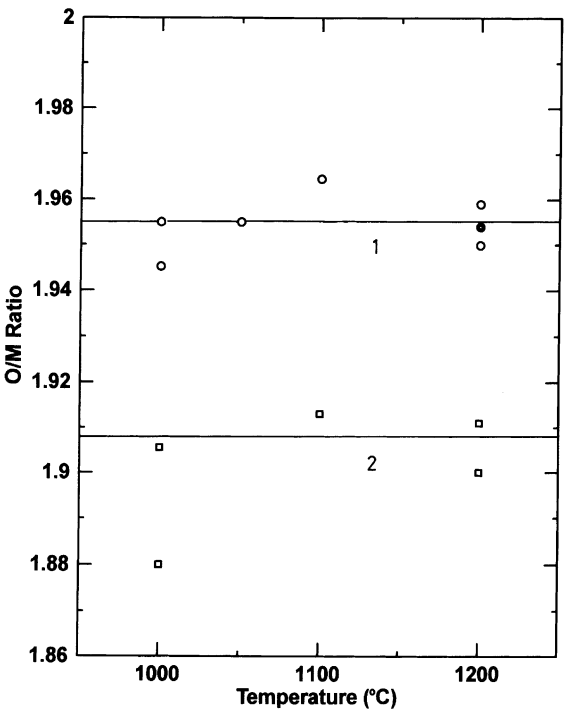

Fig. 4. O/M ratios for the steepest change of $\Delta\bar{G}_{O_2}$ (GOM) for $Mg_yEu_zU_{1-y-z}O_{2+x}$ plotted against temperature. Line 1, (○) $y = 0.05$ $z = 0.05$; (●) $y = 0.05$, $z = 0.1$; Line 2, (□) $y = 0.1$, $z = 0.05$.

In Fig. 4, the GOM values do not seem to show any correlation with temperature in the range 1000–1200°C, though the obtained values are fairly largely scattered, probably caused by difficulties in attaining equilibrium. This is sometimes the case for the oxides of high melting points sintered as pellets. The large difference in the two data at 1000°C for $y = 0.1$, $z = 0.05$ solid solution is supposed to reflect the low rearrangement rate of magnesium atoms from the substitutional to interstitial position at a lower temperature of 1000°C. A similar result has been obtained also for magnesium–gadolinium solid solution with Mg = 0.1 and Gd = 0.142 at 1000°C but not for solid solution with Mg = 0.03 or 0.06, Gd = 0.142. It is likely that longer reaction time is needed for equilibrium of solid solutions with high magnesium concentrations.

The GOM value for $y = 0.05$, $z = 0.1$ solid solution can be regarded as the same as that for $y = 0.05$, $z = 0.05$ solid solution. It is 1.955 from Fig. 4. The GOM value for $y = 0.1$, $z = 0.05$ solid solution is 1.908. These O/M ratios can be compared with those of the magnesium–gadolinium solid solutions with Gd = 0.142 [8]. For magnesium–gadolinium solid solutions, GOM did not change with temperature and the O/M ratios were 1.968, 1.940 and 1.914 for Mg = 0.03, 0.06 and 0.1, respectively. A plot of these GOMs was made as a function of magnesium concentration, which is shown in Fig. 5. The magnesium concentration (y) dependence of GOM is seen to be represented as a straight line (solid line). The result indicates that the second foreign metal

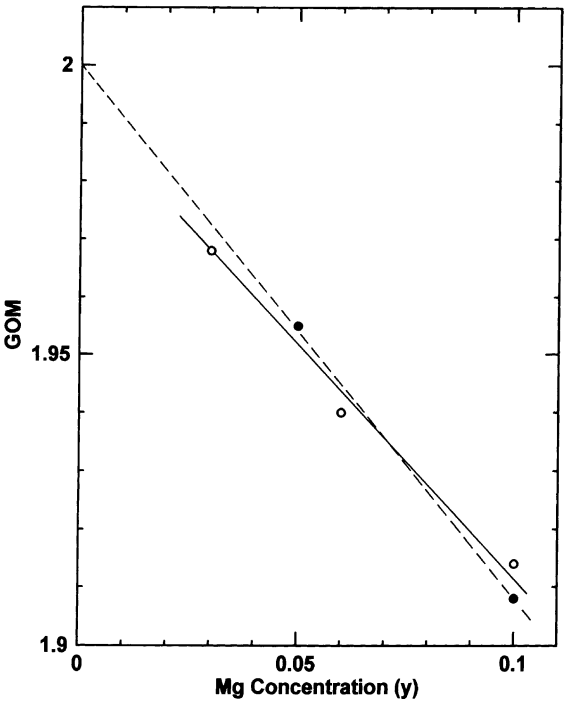

Fig. 5. GOM as a function of Mg^{2+} concentration in quaternary solid solutions. (●) magnesium–europium solid solution; (○) magnesium–gadolinium solid solution; Solid straight line: most probable line; Broken line: explicit line.

(gadolinium or europium) exerts only a small effect on GOM. It seems that europium is mainly trivalent in this quaternary solid solution at the oxygen partial pressures of Table 2, although a significant fraction of divalent europium was postulated to exist in ternary solid solution, $Eu_yU_{1-y}O_{2+x}$, at GOM [15,30]. Another straight line (broken line) is that which attains (nearly) an explicit point, viz. O/M = 2.0 at $y = 0$. This line gives the following equation to express GOM as

$$\mathrm{GOM} = 2.0 - 0.925y. \quad (1)$$

3.4. Lattice parameter as a function of magnesium and europium concentrations

Using the lattice parameters and the O/M ratios of Tables 2 and 3, the averaged lattice parameters and averaged O/M ratios were calculated as shown in Table 4. The values in Table 3 were those obtained by method 1 by heating in a stream of H_2. Thus, the oxygen partial pressure was much lower than those for GOM, but since the O/M ratios of Table 3 were not so apart, its data were used for lattice parameter calculations.

The calculated lattice parameters at $x = 0$ in Table 4 were obtained from the averaged lattice parameters and the averaged O/M ratios using the relation $\partial a/\partial x = -0.101$, where a is the lattice parameter in Å unit and x is the oxygen nonstoichiometry in the formula $Mg_yEu_zU_{1-y-z}O_{2+x}$. The above value, −0.101, is that obtained for magnesium–gadolinium solid solution [8], but the value was assumed to be used also for magnesium–europium solid solution on account of close similarity between the two solid solutions.

The increase of lattice parameter due to the increase of europium concentration by 0.05 is 5.4501–5.4578 (i.e. −0.0077) Å at $x = 0$ as obtained from Table 4. Therefore, $\partial a/\partial z = -0.0077/0.05 = -0.154$ Å, which is in good agreement with the reference values of −0.144 [26] and −0.151 Å [13]. Table 4 also shows that the increase of magnesium concentration from 0.05 to 0.1 results in an increase of lattice parameter by 5.4498–5.4578 (i.e. −0.0081) Å. Then, the rate of the lattice

Table 3
O/M ratios and lattice parameters of the solid solutions formed by heating under low oxygen pressure of dry H_2 streams ($p_{O_2} = 10^{-14}$–10^{-16} Pa) at 1000°C for 4 days (Heating number: 6; $\Delta\bar{G}_{O_2} = -463$ to -512 kJ mol^{-1})

Mg (y)	Eu (z)	O/M ratio	Lattice parameter (Å)	Remarks[a]
0.05	0.05	1.958	5.4623 ± 0.0001	S, s
0.1	0.05	1.904	5.4604 ± 0.0002	S, sb
0.05	0.1	1.931	5.4545 ± 0.0002	F2, sb

[a] S: Fluorite single phase with no MgO precipitation, F2: Fluorite two phases, s: Sharp X-ray diffraction peaks, sb: Somewhat broad X-ray diffraction peaks.

Table 4
Averaged lattice parameters, O/M ratios and calculated lattice parameters of magnesium–europium solid solutions at $x = 0$

Mg (y)	Eu (z)	Averaged lattice parameter (Å)	Averaged O/M ratio	Calculated lattice parameter at $x = 0$ (Å)
0.05	0.05	5.4623	1.955	5.4578
0.1	0.05	5.4594	1.908	5.4497
0.05	0.1	5.4546	1.955	5.4501

parameter increase by magnesium addition should be $\partial a/\partial y = -0.162$ Å. This rate is largely discrepant from the rate of increase of the lattice parameter by the substitutional magnesium, −0.5677 Å [6]. The reason may be that the magnesium ions partly migrated into the interstitial position. If we take +0.290 Å as the $\partial a/\partial y$ factor for the interstitial magnesium [8], a formula

$$0.290m - 0.5677(1-m) = -0.162 \quad (2)$$

would hold, where m stands for the ratio of interstitial magnesium to the total magnesium in the solid solution. Eq. (2) gives the m value of 0.473.

3.5. Defects and clusters in the solid solution

If the m fraction of magnesium atoms locates the interstitial position in the crystal, the formula $Mg_y^{2+}Eu_z^{3+}U_{1-2x-3y-2z}^{4+}U_{2x+2y+z}^{5+}O_{2+x}^{2-}$ is rewritten more precisely as

$$(1-my)Mg_{\frac{(1-m)y}{1-my}}^{2+}Eu_{\frac{z}{1-my}}^{3+}U_{\frac{1-2x-3y-2z}{1-my}}^{4+}U_{\frac{2x+2y+z}{1-my}}^{5+}\left\{Mg_{\frac{my}{1-my}}^{2+}\right\}O_{\frac{2+x}{1-my}}^{2-} \quad (3)$$

where the braces indicate the interstitial magnesium. The rate of lattice parameter change with oxygen amount, −0.101, suggests that the state of oxygen nonstoichiometry in Eq. (3) is hyperstoichiometric, i.e.

$$\frac{2+x}{1-my} > 2, \quad (4)$$

since if hypostoichiometric, the rate should be in the range from −0.2 to −0.3 [23]. That is to say, at GOM the solid solution is hyperstoichiometric. It does not mean, however, that the O/M ratio is higher than 2 at this point. The O/M ratio is much lower than 2. This complication comes from the fact that a part of magnesium ions occupy the interstitial sites in the fluorite lattice, which may be due to smaller crystal radius of divalent magnesium [27]. Usual type solid solutions, for example, plutonium–uranium mixed oxides, have a relatively wide region of hypostoichiometry below GOM [28,29]. The steepest change of $\Delta\bar{G}_{O_2}$ occurs at oxygen stoichiometry. For the present quaternary solid solution containing magnesium, on the other hand, the rearrangement of magnesium from substitutional sites to interstitial sites preferentially occurs before yielding oxygen hypostoichiometry. The decrease of O/M ratio occurs when the oxygen partial pressure lowers. Such a decrease in the O/M ratio is realized also by the above rearrangement.

The essential characteristics causing the GOM shift for the magnesium–europium solid solution (and also for magnesium–gadolinium solid solution) are considered to be in the manner of cluster formation of Mg^{2+} and U^{5+}. Because the GOM shift of $Eu_yU_{1-y}O_{2+x}$ solid solution, in which all europium ions locate in the substitutional position, was well explained by assuming the formation of Eu^{2+}–U^{5+} and U^{5+}–Eu^{2+}–U^{5+} clusters [31,32], it is clear that the interstitial cations are not responsible, at least mainly, for the GOM shift of the solid solutions with divalent foreign metals. In Table 5, the ion concentrations of the magnesium–europium solid solutions at GOM are listed. It may be marked from the table that the fractions of oxidized uranium, U^{5+}, are still not very low at the GOM points. Calculation of $\Delta\bar{S}_{O_2}$ and $\Delta\bar{G}_{O_2}$ through configurational entropy change for quarternary solid solution $Mg_y^{2+}Ln_z^{3+}U_{1-y-z}O_{2+x}$, where Ln is the trivalent lanthanide element, has been carried out theoretically [32]. According to this result, the following relation holds at GOM:

$$\alpha \times (Mg^{2+}\text{ fraction}) + \beta \times (Ln^{3+}\text{ fraction}) = (U^{5+}\text{ fraction}), \quad (5)$$

where α and β are the averaged numbers of U^{5+} ions bonded to one Mg^{2+} ion and one Ln^{3+} ion, respectively. There is no established method to obtain the above α and β values experimentally. However, if these values do not change largely with solid solutions of different magnesium and europium concentrations, their approximate values are obtained by solving the simultaneous equations written from Eq. (5) using the Mg^{2+}, Eu^{3+} and U^{5+} fractions of Table 5 for three different solid solutions. Three equations were obtained from Table 3, from which three sets of simultaneous equations could be constructed. These equations gave the α values ranging from 0.12 to 0.14, while all these equations gave the β values very close to 1. If it was assumed that only the substitutional Mg^{2+} ions form the clusters,

Table 5
Ion fractions in magnesium–europium solid solutions

Mg (y)	Eu (z)	Non-stoichiometry (x)	Sub. Mg^{2+} [a] $\frac{(1-m)y}{1-my}$	Int. Mg^{2+} [a] $\frac{my}{1-my}$	Eu^{3+} $\frac{z}{1-my}$	U^{4+} $\frac{1-2x-3y-2z}{1-my}$	U^{5+} $\frac{2x+2y+z}{1-my}$
0.05	0.05	−0.045	0.02699	0.02422	0.05121	0.86035	0.06145
0.1	0.05	−0.092	0.05532	0.04965	0.05248	0.82292	0.06928
0.05	0.1	−0.045	0.02699	0.02422	0.10242	0.75792	0.11266

[a] Sub.: Substitutional. Int.: Interstitial.

the α value was increased to 0.23–0.38 with the β values very close to 1. These α values are still very small, if these values are compared with the α values for ternary magnesium solid solution, $Mg_yU_{1-y}O_{2+x}$, because they were 1.50–1.56 ($y = 0.02$–0.05) [30] for this solid solution. In the case where only the interstitial Mg^{2+} ions form the clusters, the α values are not so changed from the substitutional case, i.e. $\alpha = 0.25$–0.42. It is not so realistic that divalent europium ions are present together with fairly high concentrations of U^{5+} ions (Table 5) in the magnesium–europium solid solution in the vicinity of GOM. The larger fractions of Eu^{2+} ions are supposed to emerge at much lower O/M ratios than GOM. But let us assume this state for comparison at GOM. Calculation shows $\alpha = 0.12$–0.20 and $\beta = 2.0$ in this case. This β value exhibits that the formation of U^{5+}–Eu^{2+}–U^{5+} cluster is complete. The above calculated results show that the formation ratios of the clusters by Mg^{2+} and U^{5+} are very low in any case, which yields the large leftward shift in the curves of $\Delta\bar{G}_{O_2}$ vs. O/M ratio for this quaternary solid solution. The relation between the α value and leftward shift has been studied elsewhere [30–32]. Such low ratios do not change largely with the oxidation state of europium, in sharp contrast to the clusters of Eu^{3+} (or Eu^{2+}) and U^{5+} ions which are almost completely formed. The crystals of magnesium–europium solid solution are assumed to be in a much disarranged state resulting in the formation of mostly europium clusters. That is to say, for the magnesium ions, which would be more displaced than europium ions from the normal lattice sites, the formation of the clusters with U^{5+} to sufficiently high ratios might hardly be made. This is the case also for magnesium–gadolinium solid solution [8].

References

[1] J.S. Anderson, K.D.B. Johnson, J. Chem. Soc. (1953) 1731.
[2] T. Fujino, J. Tateno, H. Tagawa, J. Solid State Chem. 24 (1978) 11.
[3] J. Tateno, T. Fujino, H. Tagawa, J. Solid State Chem. 30 (1979) 265.
[4] T. Fujino, K. Naito, J. Inorg. Nucl. Chem. 32 (1970) 627.
[5] S. Kemler-Sack, W. Rüdorff, Z. Anorg. Allg. Chem. 354 (1967) 255.
[6] T. Fujino, S. Nakama, N. Sato, K. Yamada, K. Fukuda, H. Serizawa, T. Shiratori, J. Nucl. Mater. 246 (1997) 150.
[7] T. Fujino, N. Sato, K. Yamada, J. Nucl. Mater. 247 (1997) 265.
[8] T. Fujino, N. Sato, K. Yamada, M. Okazaki, K. Fukuda, H. Serizawa, T. Shiratori, J. Nucl. Mater. 289 (2001) 270.
[9] B.E. Ingleby, K. Hand, in: I.J. Hastlings (Ed.), Advances in Ceramics, vol. 17, Fission-Product Behavior in Ceramic Oxide Fuel, American Ceramic Society, Columbus, OH, 1986, p. 57.
[10] P.T. Sawbridge, C. Baker, R.M. Cornell, K.W. Jones, D. Reed, J.B. Ainscough, J. Nucl. Mater. 95 (1980) 119.
[11] S. Kashibe, K. Une, H. Masuda, in: Proc. 1996 Spring Meeting of Atomic Energy Soc. Japan, Osaka, March 27–29, 1996, p. K35.
[12] T. Fujino, J. Nucl. Mater. 154 (1988) 14.
[13] T. Fujino, K. Ouchi, Y. Mozumi, R. Ueda, H. Tagawa, J. Nucl. Mater. 174 (1990) 92.
[14] L.N. Grossman, J.E. Lewis, D.M. Rooney, J. Nucl. Mater. 21 (1967) 302.
[15] T. Fujino, N. Sato, K. Yamada, S. Nakama, K. Fukuda, H. Serizawa, T. Shiratori, J. Nucl. Mater. 265 (1999) 154.
[16] T.B. Lindemer, J. Brynestad, J. Am. Ceram. Soc. 69 (1986) 867.
[17] R. Tanamas, KFK-1910, 1973.
[18] H.R. Hoekstra, S. Siegel, E.X. Gallagher, J. Inorg. Nucl. Chem. 32 (1970) 3237.
[19] Database MALT2, Japanese Society of Calorimetry and Thermal Analysis, 1987.
[20] D.E. Williams, Ames Lab. Rep. IS-1052, 1964.
[21] S.R. Dharwadkar, M.S. Chandrasekharaiah, Anal. Chim. Acta 45 (1969) 545.
[22] T. Fujino, T. Yamashita, Fresenius' Z. Anal. Chem. 314 (1983) 156.
[23] T. Fujino, C. Miyake, in: A.J. Freeman, C. Keller (Eds.), Handbook on the Physics and Chemistry of the Actinides, vol. 6, North-Holland, Amsterdam, 1991, p. 155.
[24] T. Fujino, K. Park, N. Sato, M. Yamada, J. Nucl. Mater. 294 (2001) 104.
[25] K. Une, M. Oguma, J. Nucl. Mater. 115 (1983) 84.
[26] T. Ohmichi, S. Fukushima, A. Maeda, H. Watanabe, J. Nucl. Mater. 102 (1981) 40.
[27] R.D. Shannon, Acta Crystallogr. A 32 (1976) 751.
[28] R.E. Woodley, J. Nucl. Mater. 96 (1981) 5.
[29] J. Edwards, R.N. Wood, G.R. Chilton, J. Nucl. Mater. 130 (1985) 505.
[30] T. Fujino, N. Sato, J. Nucl. Mater. 189 (1992) 103.
[31] T. Fujino, N. Sato, K. Yamada, J. Nucl. Mater. 223 (1995) 6.
[32] T. Fujino, N. Sato, J. Nucl. Mater. 282 (2000) 232.